ACS APPLIED MATERIALS & INTERFACES

Letter

www.acsami.org

Enhanced Light Harvesting with a Reflective Luminescent Down-Shifting Layer for Dye-Sensitized Solar Cells

Zahra Hosseini,[†] Wei-Kai Huang,[‡] Cheng-Ming Tsai,[‡] Teng-Ming Chen,[‡] Nima Taghavinia,*[,†,§] and Eric Wei-Guang Diau*[,‡,⊥]

[†]Institute for Nanoscience and Nanotechnology and [§]Physics Department, Sharif University of Technology, Tehran 14588-89694, Iran

[‡]Department of Applied Chemistry and [⊥]Institute of Molecular Science, National Chiao Tung University, Hsinchu 30010, Taiwan

Supporting Information

ABSTRACT: For a dye-sensitized solar cell with a near-infrared squaraine (SQ1) sensitizer, the photovoltaic performance was enhanced remarkably with a reflective luminescent down-shifting (R-LDS) layer to increase the light-harvesting efficiency at the wavelength region 400−550 nm where the SQ1 dye has weak absorption. Relative enhancements greater than 200% in IPCE near 500 nm and 40−54% in J_{SC} were achieved with red phosphor $CaAlSiN_3:Eu^{2+}$ as the LDS material, attaining 5.0 and 4.8% overall efficiencies of power conversion for the R-LDS layer coated on the counter electrode (front illumination) and working electrode (back illumination), respectively.

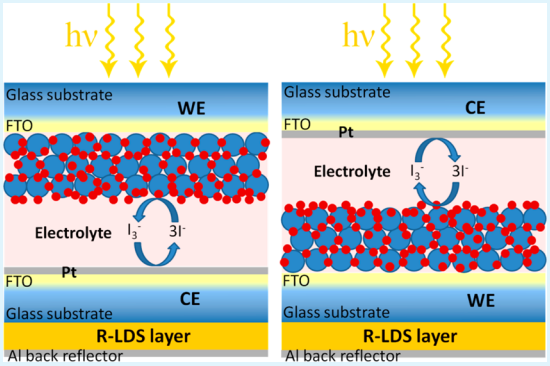

KEYWORDS: *dye-sensitized solar cells, phosphors, luminescent down shifting, squaraine dyes*

Because of their efficiency and small cost of fabrication, dye-sensitized solar cells (DSSC) are considered prospective candidates for next-generation solar cells.[1−3] In a conventional DSSC, a monolayer film of dye on a mesoporous TiO_2 layer absorbs light and injects electrons into the semiconductor. A major factor governing the performance of DSSC is the light-harvesting feature of the dye. The preferable dyes are those with the widest spectral absorbance, such as conventional polypyridyl ruthenium complexes.[4−7] The drawback of using these dyes with a wide absorption band is their small absorption coefficient, typically 5000−20 000 M^{-1} cm^{-1} for Ru-based dyes.[3] Organic dyes with large absorption coefficients, e.g., 50 000−200 000 M^{-1} cm^{-1}, typically possess narrow absorption bands.[3,8] A compromise thus exists between a spectral range of absorption and an absorption coefficient of the dyes. For dyes with a wide absorption band, a typical strategy to compensate for the small absorption coefficient of the dye is to increase the thickness of the TiO_2 mesoporous layer so that the quantity of the loaded dye can be increased to absorb a significant portion of incident photons.[9] This approach is inapplicable for solid-state or flexible DSSCs, for which the TiO_2 layer must be thin. To enhance the light-harvesting spectrum, our present work yields a new approach in employing a near-infrared (NIR) squaraine (SQ1) dye[10] with large absorption coefficients in combination with red inorganic phosphors as luminescent down-shifting (LDS) materials. The concept of using LDS materials is to shift the solar radiation effectively into the absorption band of the dye to broaden the light-harvesting range of the cell. Although this idea has been applied to different kinds of solar cells,[11,12] it is particularly helpful for DSSCs because the choice of the light-harvesting materials can be quite flexible.

Other approaches to extend the light-harvesting ability of DSSC have been reported. Among them, cosensitization with two or more dyes of separate absorption regions enhances the light-harvesting performance,[13−18] but this technically difficult[17] approach is generally limited by the unfavorable interactions between neighboring dye molecules.[19] Another approach is to use energy-relay dyes (ERD)[8,20,21] with a working principle similar to that of the LDS materials, but ERDs are limited by the requirements that they must be soluble in, but not greatly quenched by, the electrolyte media, as well as having large molar absorption coefficients.[19] Moreover, tandem cells,[19,22] being a conventional approach, considerably complicate the fabrication and increase the total cost of manufacturing.

Figure 1 illustrates the concept of LDS applied in a DSSC. The red/NIR part of the incident light is absorbed by the dye; the parts transmitted in the green and blue wavelength regions are down-shifted by the reflective LDS (R-LDS) layer to red/NIR photons and then return to the cell either directly or after reflection from the Al layer, reabsorbed by the dye molecules.

Received: April 29, 2013
Accepted: June 12, 2013
Published: June 12, 2013

   dx.doi.org/10.1021/am401584y | *ACS Appl. Mater. Interfaces* 2013, 5, 5397−5402

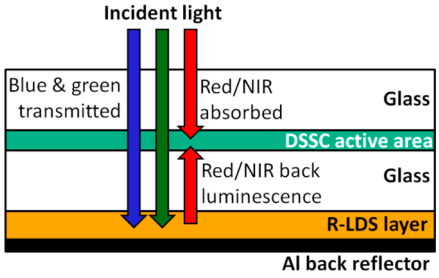

Figure 1. Scheme showing the working principle of a DSSC with a reflective layer of luminescence down-shifting materials (R-LDS). The idea is based on an active layer of the device containing a near-IR dye, which absorbs only red/NIR photons. The transmitted blue and green parts of incident light are absorbed by the phosphor in the R-LDS layer, producing the reflective red/NIR luminescent photons that match the absorption spectrum of the dye.

The R-LDS layer hence shifts photons at shorter wavelengths to photons at longer wavelengths according to normal absorption and luminescence, as reported elsewhere.[23,24] The R-LDS layer is a granular layer with a high diffuse reflectivity combined with a thin layer of Al foil, that can function as a back reflector for the red/NIR photons emitted from the LDS material bouncing back into the DSSC. The function of this reflective feature is to enhance the light-scattering effect so as to increase photocurrents, as we reported for the nanostructured platinum counter electrode (CE).[25] The diffuse reflection spectra of the R-LDS layers are shown in Figure S1 in the Supporting Information. The proposed R-LDS layer deposited with a simple powder-coating method differs conceptually from conventional transparent LDS layers with small light scattering. This condition implies that the R-LDS layer is more efficient than conventional LDS layers used in silicon solar cells.[11] R-LDS is applicable only in transparent solar cells such as DSSCs. The appropriate LDS materials should have a luminescence spectrum matching the absorption spectrum of the dye; the overlop between the emission spectrum and the excitation spectrum of the LDS materials should be minimized in order to avoid the loses due to reabsorption of the emitted photons by the luminescent species in the LDS layer. The LDS materials should also have large quantum efficiencies (QEs). Suitable candidates are inorganic phosphors, organic luminescent materials, or inorganic quantum dots.[12] We selected inorganic phosphors as our R-LDS layer because of their great QEs, excellent photochemical and thermal stabilities, low cost, and ease of processing. It is worth mentioning that deposition of the LDS layer from the phosphor powder is feasible by doctor blading, screen printing, or simply putting the pressed membrane over the cell.

Our R-LDS approach differs from those reported with luminescence down-conversion (LDC) materials. Liu et al.[26] used lanthanum vanadium oxides ($LaVO_4$) as a LDC material coated on the front surface of the working electrode (WE) to filter out the UV to improve the stable endurance of DSSC, but no enhanced short-circuit current density (J_{SC}) was achieved; Hafez et al.[27] observed a significantly enhanced J_{SC} using lanthanide-doped TiO_2 photoelectrodes with europium and samarium ions serving as LDC materials that converted UV light to visible emission for the ruthenium dye to absorb in a transparent device configuration, but the proof of the LDC layer for the photocurrent enhancement was unavailable. We placed the R-LDS layer outside the DSSC to avoid the complication of fabrication of the device. The net effect of the R-LDS layer increases the J_{SC} of the device to 54%; a remarkable efficiency, η = 5.0%, of power conversion is unprecedented for a SQ1-based DSSC.

Three Eu^{2+}-doped red phosphors served as LDS materials in the present work; their molecular formulas are $CaAlSiN_3:Eu^{2+}$ (LDS1), $Ca_2Si_5N_8:Eu^{2+}$ (LDS2) and $CaZnOS:Eu^{2+}$ (LDS3). The QE of luminescence of the phosphors, measured with an integrating sphere, are LDS1, 51%; LDS2, 42%; and LDS3, 17% (see Table S1 in the Supporting Information). The normalized excitation and emission spectra of the three LDS materials appear in Figure 2, together with the normalized absorption of

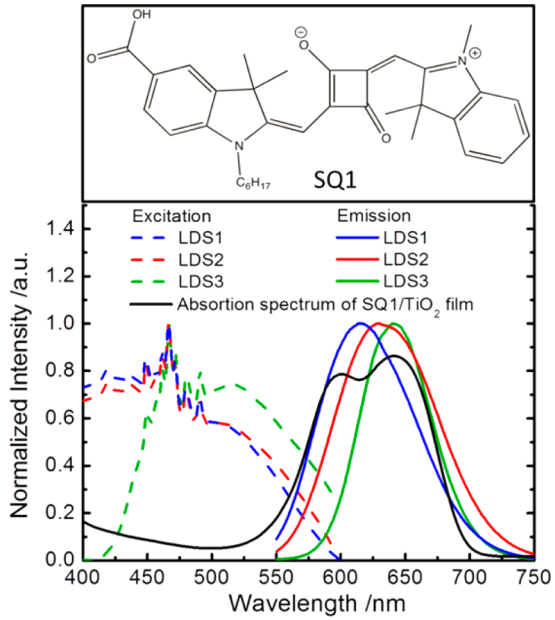

Figure 2. Normalized excitation spectra of three red phosphors (dashed curves) recorded at emission wavelengths λ_{em}/nm = 615, 630, and 650 for LDS1, LDS2, and LDS3, respectively. The normalized emission spectra of the corresponding phosphors (solid curves) were recorded at excitation wavelength λ_{ex}/nm = 466. The normalized absorption spectrum of a SQ1 (molecular structure shown on top) sensitized TiO_2 film is shown as a black solid curve.

a SQ1-sensitized TiO_2 film shown as a black trace. Nearly all emission from the phosphors can be absorbed by the SQ1 dye inside the DSSC, because of the great overlap between the emission bands of the phosphors and the absorption band of the SQ1 dye. The excitation range of the phosphors fully covers the short-wavelength part of the spectrum that is not absorbed by the SQ1-sensitized film. The solar irradiation below 550 nm can thus be absorbed by the SQ1 dye via the luminescence of the LDS materials, and the light-harvesting efficiency of DSSC improves significantly.

The free-standing R-LDS layer was made by pressing the phosphor powder at pressure 2 MPa; the layer was placed on top of the DSSC on either the CE side or WE side. These two device structures are shown in Figure 3. As the inorganic phosphors have small absorption coefficients, a thick layer of phosphor (~300 μm) is required to fully absorb photons in the range 350−550 nm. The DSSC is illuminated from the front side of the device of which the R-LDS layer is on the CE side (Figure 3a), whereas back illumination is used in the case of the R-LDS layer on the WE side (Figure 3b). The design of these two structures aims to utilize the back reflection feature of the

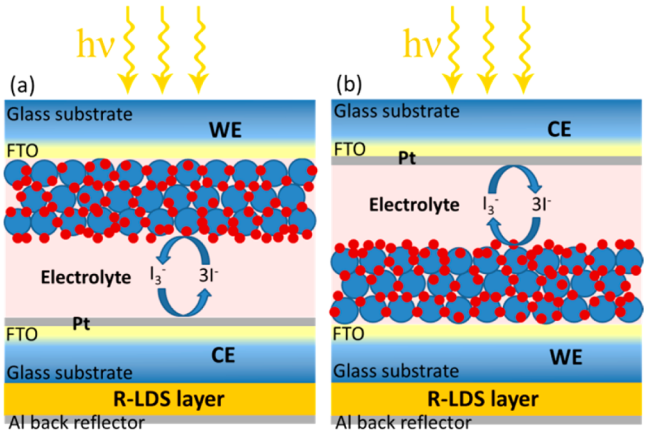

Figure 3. Schematic demonstrations of two DSSC structures containing the proposed R-LDS layer: (a) the R-LDS layer is placed on the counter- electrode (CE) side and incident light illuminated from the working electrode (WE) side (front illumination); (b) the R-LDS layer is placed on the WE side and the incident light illuminated from the CE side (back illumination).

R-LDS layers as well as their LDS effect in order to enhance the light harvesting of DSSCs not only in short wavelength spectral region where the SQ1 dye has very weak absorption, but also in the absorption range of the SQ1 dye.

There are several factors causing the current loss of the device in the present R-LDS configuration. The main loss is caused by the QE of the luminescent material used in the LDS layer, which is usually much less than unity. The effect of QE on the final enhancement of the short-circuit current density is clearly shown in the following results by comparison of different devices with different LDS layers. Another possible current losing channels are reabsorption of the emitted photons by the luminescent species itself in the LDS layer and escaping out the emitted photons through back and side parts of the LDS layer. We tried to minimize the reabsorption loss by choosing appropriate luminescent materials with almost no overlp between their absorption and emission bands. Moreover, the Al layer at the back of the LDS layer acts as a reflective medium to prevent the escape of the emitted photons from the back side of the LDS layer.

Figure 4 shows the photocurrent–voltage (J–V) characteristics of DSSC with and without the R-LDS layer on either CE or WE side measured under standard AM1.5G one-sun irradiation (100 mW cm^{-2}); the corresponding photovoltaic parameters are shown in Table 1. For both structures, the devices with the R-LDS layer have much greater J_{SC} than the reference devices without the R-LDS layer, but the open-circuit voltages (V_{OC}) and the filling factors (FF) of these devices show no significant difference (Table 1). For clarity, we define the percentage increase in short-circuit photocurrent density ΔJ_{SC}/% as $(J_{SC,LDS} - J_{SC,ref})/J_{SC,ref}$; $J_{SC,LDS}$ and $J_{SC,ref}$ represent the short-circuit current densities of devices with and without a R-LDS layer, respectively. As summarized in Table 1, ΔJ_{SC}/% attained 40, 36, and 23 for devices with LDS1, LDS2, and LDS3 coated on the CE side (front illumination), respectively, whereas the photocurrent density enhancements reached 54, 53, and 33% for those LDS materials coated on the WE side (back illumination). The ΔJ_{SC} (%) values are greater for the R-LDS layers coated on the WE side than on the CE side because of the "filter effect" caused by the electrolyte and the Pt layer.[28] The absorption spectrum of the electrolyte and the transmission spectrum of the Pt layer are shown in Figures S2 and S3 in the Supporting Information, respectively. For the back-illuminated WE-coated devices, the filter effect remains the same for the DSSC without and with R-LDS layer, but for the front illuminated CE-coated devices, the filter effect makes no contribution for the performance of the reference cell. Therefore, higher ΔJ_{SC} values were achieved for the DSSC with R-LDS layer on the WE side than those on the CE side. However, larger ΔJ_{SC} of the WE-coated devices did not improve the device performances relative to their CE-coated counterparts because the initial loss of the incident photons becomes significant under back-illumination condition for the WE-coated devices.[28]

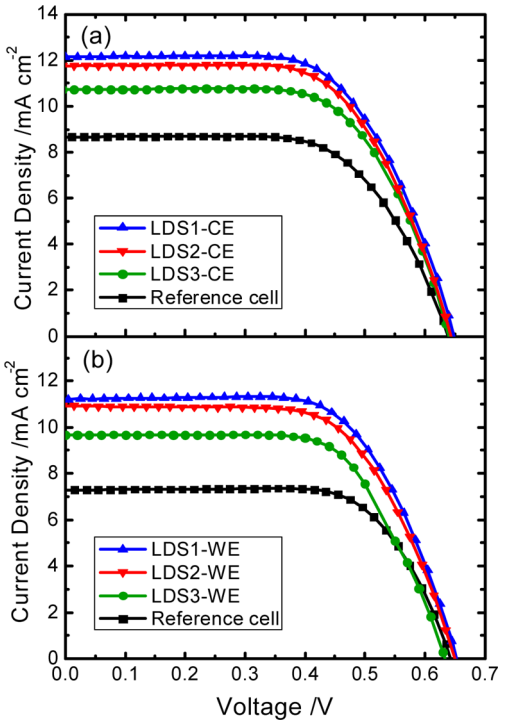

Figure 4. Current–voltage (J–V) characteristics of SQ1-based DSSC devices with the R-LDS layer containing red phosphors LDS1, LDS2 and LDS3 coated on (a) the CE side (front illumination) and (b) the WE side (back illumination); the reference cells have the same device structures as those shown in Figure 3 but without the added Al/R-LDS layer.

Table 1. Photovoltaic Parameters of SQ1-Sensitized TiO_2 Solar Cells with and without (reference cell) an Added R-LDS Layer under Standard AM 1.5G One-Sun Irradiation (100 mW cm^{-2})

device configuration	V_{OC} (mV)	J_{SC} (mA cm^{-2})	FF	η (%)	ΔJ_{SC} (%)
(front illumination)					
reference cell	641	8.68	0.641	3.6	
LDS1-CE	651	12.14	0.627	5.0	40
LDS2-CE	646	11.82	0.630	4.8	36
LDS3-CE	641	10.71	0.648	4.5	23
(back illumination)					
reference cell	645	7.25	0.698	3.3	
LDS1-WE	655	11.17	0.652	4.8	54
LDS2-WE	648	11.07	0.633	4.5	53
LDS3-WE	634	9.67	0.661	4.1	33

dx.doi.org/10.1021/am401584y | ACS Appl. Mater. Interfaces 2013, 5, 5397–5402

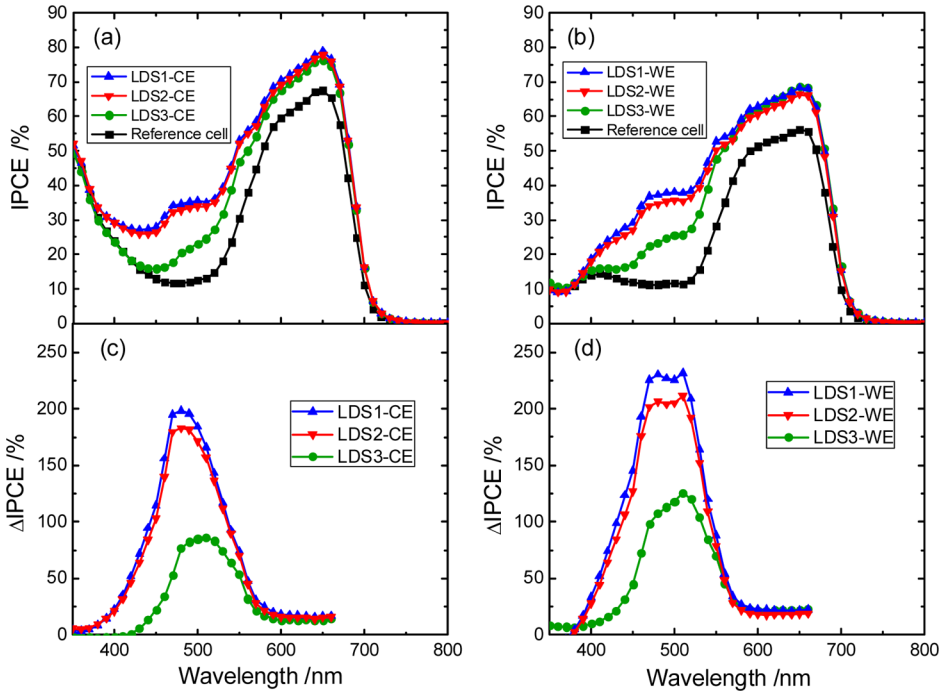

Figure 5. IPCE action spectra of devices with and without the R-LDS layer coated on either (a) the CE side or (b) the WE side, and the percentage enhancement of IPCE with respect to the reference cell (ΔIPCE) for devices with a R-LDS layer coated on either (c) the CE side or (d) the WE side.

The action spectra of efficiency of incident photons converted to current (IPCE) are shown in panels a and b in Figure 5 for devices with the R-LDS layer coated on the CE and WE sides, respectively. The IPCE results exhibit prominent enhancements in spectral range 400−550 nm coinciding with the excitation spectra of the phosphors shown in Figure 2, experimentally proving the concept of LDS applied herein. At wavelength less than 550 nm, the IPCE values of these LDS devices are significantly greater than those of their reference cells, attaining IPCE 38% near 500 nm for the WE-coated LDS1 device; this value cannot exceed 10% in a conventional DSSC sensitized with the SQ1 dye.[10,29] The greatly enhanced IPCE in wavelength range 400−550 nm was caused by the down-shifting of photons in this range to wavelengths that match the SQ1 absorption. Moreover, the R-LDS layer can act as a reflector layer to reflect the light into the DSSC to enhance the IPCE at wavelength range 550−800 nm.[25]

The remarkable LDS effect at the 400−550 nm spectral range is readily understood from Figure 5c and 5d, which show the relative enhancements in IPCE over the reference cell at each wavelength, ΔIPCE (%) = $(IPCE_{,LDS} - IPCE_{,ref})/IPCE_{,ref}$; $IPCE_{,LDS}$ and $IPCE_{,ref}$ represent the IPCE values of the devices with and without the R-LDS layer, respectively. The ΔIPCE values of the LDS1 devices attained 200 and 230% near 500 nm for the LDS1 material coated on the CE and the WE sides, respectively, whereas the ΔIPCE enhancements in the 550−800 nm range were less than 20%. ΔJ_{SC} values calculated from IPCE in the spectral ranges 350−550 and 550−800 nm are summarized in Table S2 in the Supporting Information, which confirm the dominant effect of LDS responsible for the enhancements of J_{SC}. We have also estimated the relative enhancements of the power conversion efficiencies of the three devices in the spectral ranges of 350−550 nm and 550−800 nm; the results are summarized in Table S3 in the Supporting Information. Our results indicate that the relative efficiency enhancements of the three LDS devices are quite similar in the 350−550 nm range but the enhancements of the LDS1 and LDS2 devices are much greater than those of the LDS3 devices in the 550−800 nm range. Both enhancements in photocurrents and efficiencies indicate a separate effect of the R-LDS layer, i.e., the enhancement in the 550−800 nm is mainly due to the reflective effect of the Al-foil, but the enhancement in the 350−550 nm is attributed to the LDS effect of the phorsphor to be detailed below.

The superior performance of the LDS1 device is attributed to the greater QE of luminescence of $CaAlSiN_3:Eu^{2+}$ than of $Ca_2Si_5N_8:Eu^{2+}$ and $CaZnOS:Eu^{2+}$ (see Table S1 in the Supporting Information), indicating that more absorbed photons become effectively converted to lower-energy photons, reabsorbed by the SQ1 dye to increase the current for DSSC. Our best ΔIPCE enhancement was achieved for SQ1-sensitized solar cells with LDS1 coated on the WE side under back-illumination condition (V_{OC} = 655 mV, J_{SC} = 11.17 mA cm^{-2}, FF = 0.652, and η = 4.8%), but the greatest photovoltaic performance was obtained for the same device with LDS1 coated on the CE side under a front-illumination condition (V_{OC} = 651 mV, J_{SC} = 12.14 mA cm^{-2}, FF = 0.627, and η = 5.0%). For those cells relative to their uncoated counterparts (reference cells), the relative enhancements in device performance are remarkable: 39% (η = 5.0 vs 3.6%) and 45% (η = 4.8 vs 3.3%) for the CE-coated front-illuminated and the WE-coated back-illuminated devices, respectively. The observed enhancements are much greater than the reported 26% enhancement (η = 3.21 vs 2.55%) with an ERD (PTCDI) to enhance the light-harvesting performance of devices sensitized with a zinc phthalocyanine dye (TT1).[8] Relative to the SQ1-sensitized system, the device performance enhanced only ∼5% (η = 3.67 vs 3.51%) was reported with a phosphorescent ruthenium complex as an ERD.[18] With the great performance in short-circuit current density over 12 mA cm^{-2} using our R-

LDS concept, the performance of the CE-coated LDS1 device has been improved to η = 5.0%, which is an outstanding result for a DSSC sensitized with only the SQ1 dye.

In conclusion, we present here a proof of concept of applying luminescent down-shifting (LDS) materials in a reflective configuration to enhance significantly the photovoltaic performance for mesoporous TiO_2 solar cells sensitized with a near-infrared squaraine dye (SQ1). Three Eu^{2+}-doped red phosphors were selected as potential LDS materials such that their emission spectra matched well the absorption spectrum of SQ1. $CaAlSiN_3:Eu^{2+}$ (LDS1) with the best luminescence quantum yield (QE = 0.51) exhibited relative enhancements of IPCE achieving 200 and 230% near 500 nm for LDS1 coated on the counter-electrode side (front illumination) and the working-electrode side (back illumination), respectively, fabricated outside the DSSC. Accordingly, relative enhancements of η (or J_{SC}) of the corresponding devices attained 39% (or 40%) and 45% (or 54%) for the former and the latter, respectively, giving overall efficiency ~5% of power conversion, which becomes a record for a SQ1-sensitized solar cell. The concept of applying an R-LDS layer to enhance the light-harvesting performance of DSSC can be further designed in selecting an appropriate sensitizer among many well studied dyes. The R-LDS layers exhibit a bifunctional characteristic showing the energy down-shifting and light backscattering features, which might be utilized in photon-management techniques. Finally, this approach is particularly helpful in cases in which the available surface area for dye sensitization is limited, such as in solid-state DSSC[30−32] and flexible devices;[33−35] work in this direction is in progress.

METHODS

Polycrystalline phosphor $CaZnOS:Eu^{2+}$ (LDS3) was prepared with a solid-state reaction. CaS (99.9%), ZnO (99.99%) and Eu_2O_3 (99.9%) (all from Aldrich Chemicals, Milwaukee, WI, USA) were weighed in stoichiometric proportions and ground intimately. The mixture was then sintered under a reducing atmosphere at 900 °C for 8 h and cooled to 23 °C in an electric furnace.[36] Phosphors $CaAlSiN_3:Eu^{2+}$ (LDS1) and $Ca_2Si_5N_8:Eu^{2+}$ (LDS2) (Taiwan Nakamura Scientific Instruments Corporation) and SQ1 dye (Luminescence Technology Corporation, Taiwan) were obtained as indicated. Optical absorbance and quantum efficiency of phosphor samples were measured with an integrating sphere method.[36]

A paste of TiO_2 nanoparticles (particle size 20 nm) was prepared with a combined sol−gel/hydrothermal method.[9] The TiO_2 films (active area 0.4 × 0.4 cm^2, thickness ~10 μm) were prepared with repetitive screen printing of TiO_2 paste on a FTO glass substrate (TEC15, Hartford, USA), then annealed according to a standard programmed procedure.[9] The annealed films were treated with $TiCl_4$ fresh aqueous solution (40 mM) at 70 °C for 30 min. After sintering at 500 °C for 30 min, the TiO_2 films were sensitized in a SQ1 solution (0.2 mM) in ethanol containing chenodeoxycholic acid (CDCA, 20 mM) for 90 min. The counter electrode was Pt-deposited FTO glass fabricated with thermal decomposition.[25] The dye-sensitized working electrode was assembled with the Pt-coated counter electrode into a cell of sandwich type and sealed with a hot-melt film (Surlyn, thickness 30 μm) under thermal compression. The electrolyte injected into the device consists of butyl methyl imidazolium iodide (0.6 M), iodine (0.01 M), lithium iodide (0.1 M), guanidinium thiocyanate (0.10 M), and 4-tertbutylpyridine (0.5 M) in a mixture of acetonitrile and valeronitrile (v:v = 85: 15). The free-standing R-LDS layers were made by pressing the phosphor powder at pressure 2 MPa. The layers and the Al foil layer at back are then fixed by a holder made of plexi-glass and placed on top of the DSSC on either the CE side or the WE side.

Excitation and emission spectra of phosphors were recorded (Spex Fluorolog-3 spectrofluorometer, Instruments S.A., Edison, N.J., USA) equipped with a Xe light source (450 W) and double excitation monochromators. Photovoltaic measurements were made with a solar simulator (AM 1.5G, XES-40S1, SAN-EI), calibrated with a standard Si reference cell (Oriel PN 91150 V, VLSI standards). $J-V$ curves were measured with a source meter (Keithley 2400, computer-controlled) for all devices with an external shadow mask (area 0.5 × 0.5 cm^2). The efficiencies of conversion of incident photons to current (IPCE) of the devices were measured with a system comprising a Xe lamp (A-1010, PTi, 150 W), monochromator (PTi, 1200 grooves mm^{-1} blazed at 500 nm), and source meter (Keithley 2400).

ASSOCIATED CONTENT

Supporting Information

Diffuse reflection spectra (DRS) of R-LDS layers, absorption spectrum of the electrolyte, transmission spectrum of the Pt electrode, QE and relative absorbance of phosphors used in R-LDS layers, relative increase/% in short circuit current density of the devices in two wavelength range and relative increase/% in power conversion efficiency of the devices caused by down shifting of photons ($\Delta\eta_{DS}$) and by reflection of transmitted photons ($\Delta\eta_R$). This material is available free of charge via the Internet at http://pubs.acs.org/.

AUTHOR INFORMATION

Corresponding Author

*E-mail: taghavinia@sharif.edu (N.T.); diau@mail.nctu.edu.tw (E.W-.G.D.).

Notes

The authors declare no competing financial interest.

ACKNOWLEDGMENTS

This work is supported by Iranian Nanotechnology Initiative Council, and National Science Council of Taiwan and Ministry of Education of Taiwan under the ATU program. Z.H. thanks National Chiao Tung University (Hsinchu, Taiwan) and Iranian Ministry of Science and Technology for support of her visit to NCTU.

REFERENCES

(1) O'Regan, B.; Grätzel, M. *Nature* **1991**, *353*, 737−740.
(2) Grätzel, M. *Nature* **2001**, *414*, 338−344.
(3) Hagfeldt, A.; Boschloo, G.; Sun, L.; Kloo, L.; Pettersson, H. *Chem. Rev.* **2010**, *110*, 6595−6663.
(4) Nazeeruddin, M. K.; De Angelis, F.; Fantacci, S.; Selloni, A.; Viscardi, G.; Liska, P.; Ito, S.; Takeru, B.; Grätzel, M. *J. Am. Chem. Soc.* **2005**, *127*, 16835−16847.
(5) Wang, Q.; Ito, S.; Grätzel, M.; Fabregat-Santiago, F.; Mora-Seró, I.; Bisquert, J.; Bessho, T.; Imai, H. *J. Phys. Chem. B* **2006**, *110*, 25210−25221.
(6) Chen, C.-Y.; Wang, M.; Li, J.-Y.; Pootrakulchote, N.; Alibabaei, L.; Ngoc-le, C.-H.; Decoppet, J.-D.; Tsai, J.-H.; Grätzel, C.; Wu, C.-G.; Zakeeruddin, S. M.; Grätzel, M. *ACS Nano* **2009**, *3*, 3103−3109.
(7) Yu, Q.; Wang, Y.; Yi, Z.; Zu, N.; Zhang, J.; Zhang, M.; Wang, P. *ACS Nano* **2010**, *4*, 6032−6038.

(8) Hardin, B. E.; Hoke, E. T.; Armstrong, P. B.; Yum, J.; Comte, P.; Torres, T.; Frechet, J. M. J.; Nazeeruddin, K.; Gratzel, M.; McGehee, M. D. *Nat. Photonics* **2009**, *3*, 406−411.
(9) Shiu, J.-W.; Lan, C.-M.; Chang, Y.-C.; Wu, H.-P.; Huang, W.-K.; Diau, E. W.-G. *ACS Nano* **2012**, *6*, 10862−10873.
(10) Yum, J.-H.; Walter, P.; Huber, S.; Rentsch, D.; Geiger, T.; Nüesch, F.; De Angelis, F.; Grätzel, M.; Nazeeruddin, M. K. *J. Am. Chem. Soc.* **2007**, *129*, 10320−10321.
(11) Bettiol, F.; Richards, B. S.; McIntosh, K. R.; Lau, G.; Cotsell, J. N.; Hanton, K. *Prog. Photovolt: Res. Appl.* **2009**, *17*, 191−197.
(12) Klampaftis, E.; Ross, D.; McIntosh, K. R.; Richards, B. S. *Sol. Energy Mater. Sol. Cells* **2009**, *93*, 1182−1194.
(13) Lan, C.-M.; Wu, H.-P.; Pan, T.-Y.; Chang, C.-W.; Chao, W.-S.; Chen, C.-T.; Wang, C.-L.; Lin, C.-Y.; Diau, E. W.-G. *Energy Environ. Sci.* **2012**, *5*, 6460−6464.
(14) Yella, A.; Lee, H.-W.; Tsao, H. N.; Yi, C.; Chandiran, A. K.; Nazeeruddin, M. K.; Diau, E. W.-G.; Yeh, C.-Y.; Zakeeruddin, S. M.; Grätzel, M. *Science* **2011**, *334*, 629−634.
(15) Ehret, A.; Stuhl, L.; Spitler, M. T. *J. Phys. Chem. B* **2001**, *105*, 9960−9965.
(16) Ogura, R. Y.; Nakane, S.; Morooka, M.; Orihashi, M.; Suzuki, Y.; Noda, K. *Appl. Phys. Lett.* **2009**, *94*, 073308−073310.
(17) Wu, H.-P.; Ou, Z.-W.; Pan, T.-Y.; Lan, C.-M.; Huang, W.-K.; Lee, H.-W.; Reddy, N. M.; Chen, C.-T.; Chao, W.-S.; Yeh, C.-Y.; Diau, E. W.-G. *Energy Environ. Sci.* **2012**, *5*, 9843−9848.
(18) Li, L.-L.; Diau, E. W.-G. *Chem. Soc. Rev.* **2013**, *42*, 291−304.
(19) Yum, J.-H.; Baranoff, E.; Wenger, S.; Nazeeruddin, M. K.; Grätzel, M. *Energy Environ. Sci.* **2011**, *4*, 842−857.
(20) Yum, J.-H.; Baranoff, E.; Hardin, B. E.; Hoke, E. T.; McGehee, M. D.; Nüesch, F.; Grätzel, M.; Nazeeruddin, M. K. *Energy Environ. Sci.* **2010**, *3*, 434−437.
(21) Yum, J.-H.; Hardin, B. E.; Moon, S.-J.; Baranoff, E.; Nüesch, F.; McGehee, M. D.; Grätzel, M.; Nazeeruddin, M. K. *Angew. Chem., Int. Ed.* **2009**, *48*, 9277−9280.
(22) Bremner, S. P.; Levy, M. Y.; Honsberg, C. B. *Prog. Photovolt: Res. Appl.* **2008**, *16*, 225−233.
(23) Hovel, H. J.; Hodgson, R. T.; Woodall, J. M. *Sol. Energy Mater.* **1979**, *2*, 19−29.
(24) Huang, X.; Han, S.; Huang, W.; Liu, X. *Chem. Soc. Rev.* **2013**, *42*, 173−201.
(25) Li, L.-L.; Chang, C.-W.; Wu, H.-H.; Shiu, J.-W.; Wu, P.-T.; Wei-Guang Diau, E. *J. Mater. Chem.* **2012**, *22*, 6267−6273.
(26) Liu, J.; Yao, Q.; Li, Y. *Appl. Phys. Lett.* **2006**, *88*, 173119−173122.
(27) Hafez, H.; Saif, M.; Abdel-Mottaleb, M. S. a. *J. Power Sources* **2011**, *196*, 5792−5796.
(28) Li, L.-L.; Chen, Y.-J.; Wu, H.-P.; Wang, N. S.; Diau, E. W.-G. *Energy Environ. Sci.* **2011**, *4*, 3420−3425.
(29) Yum, J. H.; Moon, S. J.; Humphry-Baker, R.; Walter, P.; Geiger, T.; Nüesch, F.; Grätzel, M.; Nazeeruddin, M. D. K. *Nanotechnology* **2008**, *19*, 424005.
(30) Bach, U.; Comte, P.; Moser, J. E.; Weisso, F.; Gratzel, M. *Nature* **1998**, *395*, 583−585.
(31) Snaith, H. J.; Schmidt-Mende, L. *Adv. Mater.* **2007**, *19*, 3187−3200.
(32) Snaith, H. J.; Humphry-Baker, R.; Chen, P.; Cesar, I.; Zakeeruddin, S. M.; Grätzel, M. *Nanotechnology* **2008**, *19*, 424003.
(33) Dürr, M.; Schmid, A.; Obermaier, M.; Rosselli, S.; Yasuda, A.; Nelles, G. *Nat. Mater.* **2005**, *4*, 607−611.
(34) Ito, S.; Ha, N.-L. C.; Rothenberger, G.; Liska, P.; Comte, P.; Zakeeruddin, S. M.; Péchy, P.; Nazeeruddin, M. K.; Grätzel, M. *Chem. Commun.* **2006**, 4004−4006.
(35) Yamaguchi, T.; Tobe, N.; Matsumoto, D.; Nagai, T.; Arakawa, H. *Sol. Energy Mater. Sol. Cells* **2010**, *94*, 812−816.
(36) Kuo, T.-W.; Liu, W.-R.; Chen, T.-M. *Opt. Express* **2010**, *18*, 8187−8192.